Modelling-robustness of the past and future forced changes of the ENSO-Indian summer monsoon teleconnection

Aneesh Sundaresan[1, 2*], Tamas Bodai[1, 2], June-Yi Lee[1, 2],

[1] IBS Center for Climate Physics, Busan, South Korea

[2] Pusan National University, Busan, South Korea

aneesh.ply@gmail.com

26/07/2022

ENSO-Indian Summer Monsoon Teleconnection

- In India, the summer monsoon period begins in the late May or early June and lasts up to September, bringing nearly 75% of country's annual rainfall.
- The interannual variability of the Indian Summer Monsoon (ISM) is strongly associated with the El Niño Southern Oscillation (ENSO).
- In general, El Niño (La Niña) years are associated with above (below) normal ISM rainfall.
- Most of the severe droughts occur over the Indian region are during El Niño years while there have been drought years without El Niño.

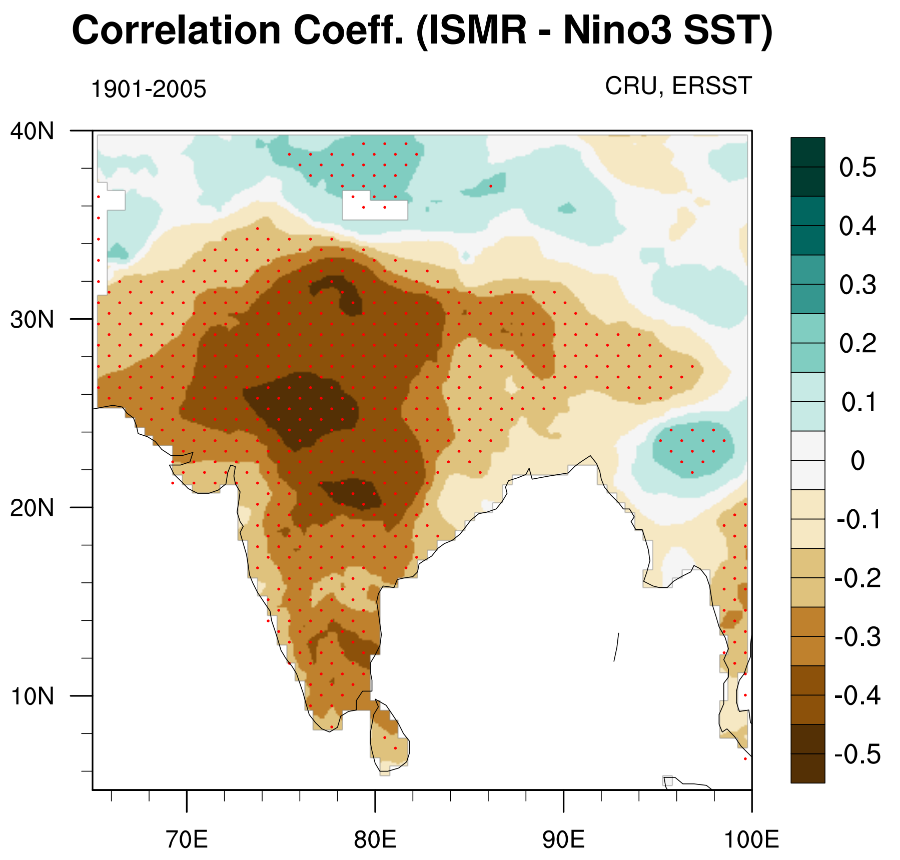

- The inverse relationship between El Niño and ISM weakened in the recent decades, particularly after 1970s [*Kumar et al.*, 1999]. They argued that the weakening is mainly due to rise in the Eurasian surface temperature during winter and summer, and shifting of the Walker cell towards south-eastward direction.
- Recent studies linked the weakening of the teleconnection to global warming, AMO, PDO, co-occurrence of El Nino and IOD events, shift in the ENSO's center of action etc

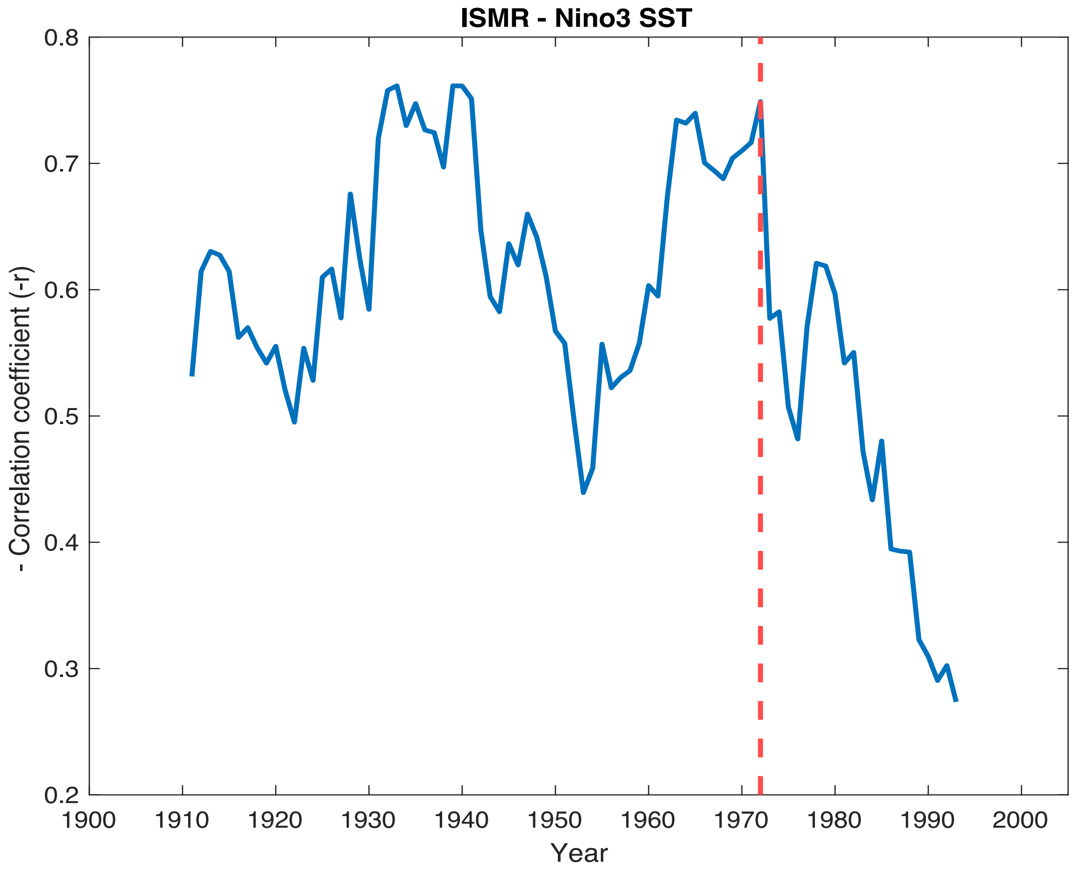

Fig: displays the time-evolution of 21 year window moving correlation coefficients (r), between Nino3 SST and ISM rainfall.

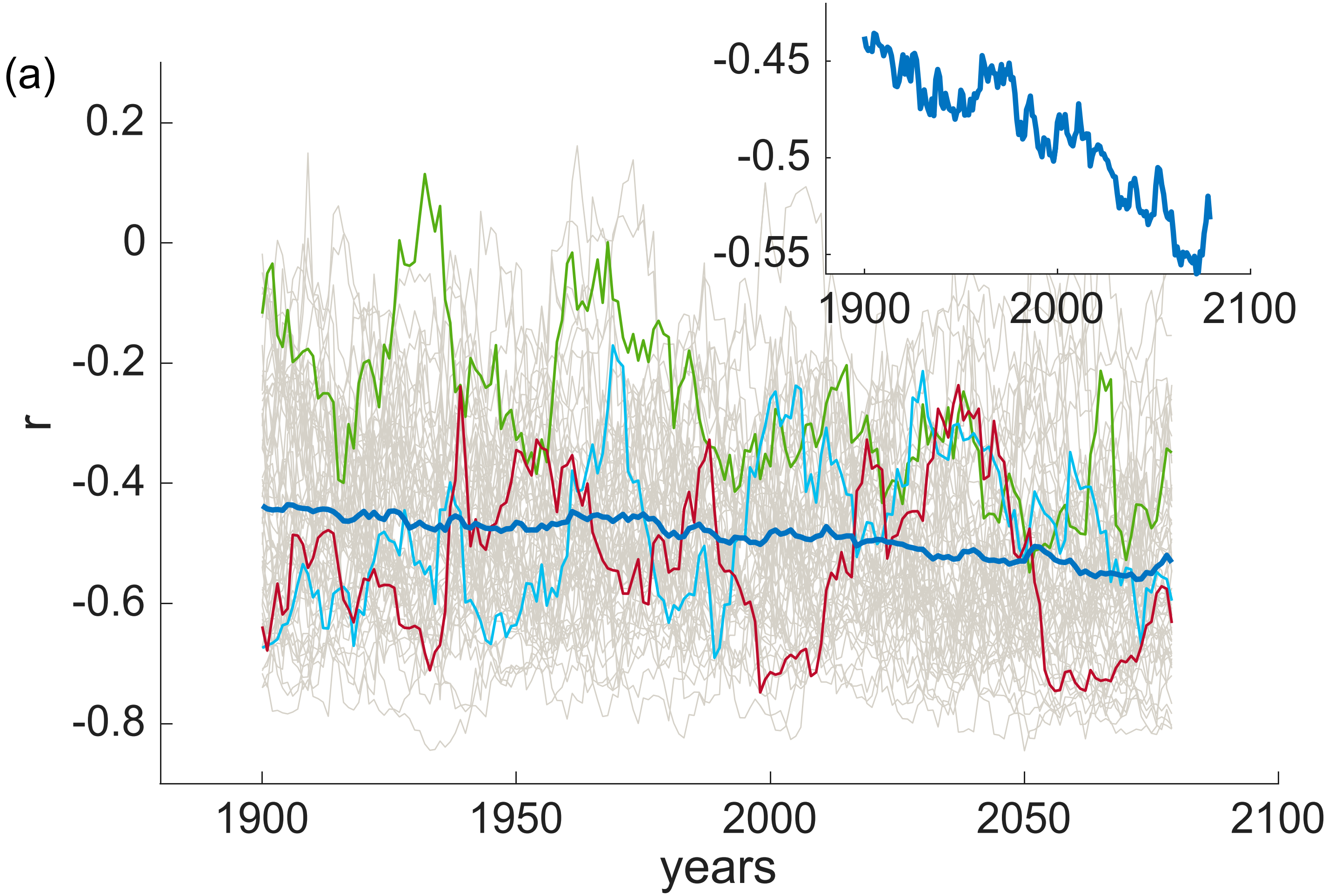

Fig: Moving temporal correlation coefficient (between Nino3 SST and ISM rainfall) for the MPI-GE in the historical period and RCP8.5 forcing scenario. The thin gray lines show all the realizations while three realizations are shown in color, providing examples. Thick blue lines show the ensemble average of the temporal correlation, which are blown up in insets to better indicate any trend.

Bodai et al., 2020, J. Cli

The teleconnection strength is typically increasing on the long term in view of appropriately revised ensemble-wise indices.

Bodai et al., 2020, J. Cli

Objective

Study the forced response of the teleconnection between the ENSO and the Indian Summer Monsoon (ISM) in a multi-model ensemble of initial conditional ensembles under historical forcing and future forcing scenarios.

Model	No. of Members	Period	Scenario
CESM2	100	1850-2100	SSP 3-7.0
MPI-ESM	63	1850-2100	RCP 8.5
MIROC6	50	1850-2100	SSP5-8.5
CanESM5	50	1850-2100	SSP5-8.5
CanESM2	50	1950-2100	RCP 8.5
CSIRO-MK3.6	30	1850-2100	RCP 8.5
GFDL ESM2M	30	1950-2100	RCP 8.5

Table: 1

The forced response of the teleconnection, or a characteristic of it, is defined as the time dependence of a correlation coefficient evaluated over the ensemble.

The Forced Evolution of Correlation Coefficients: Historical Period

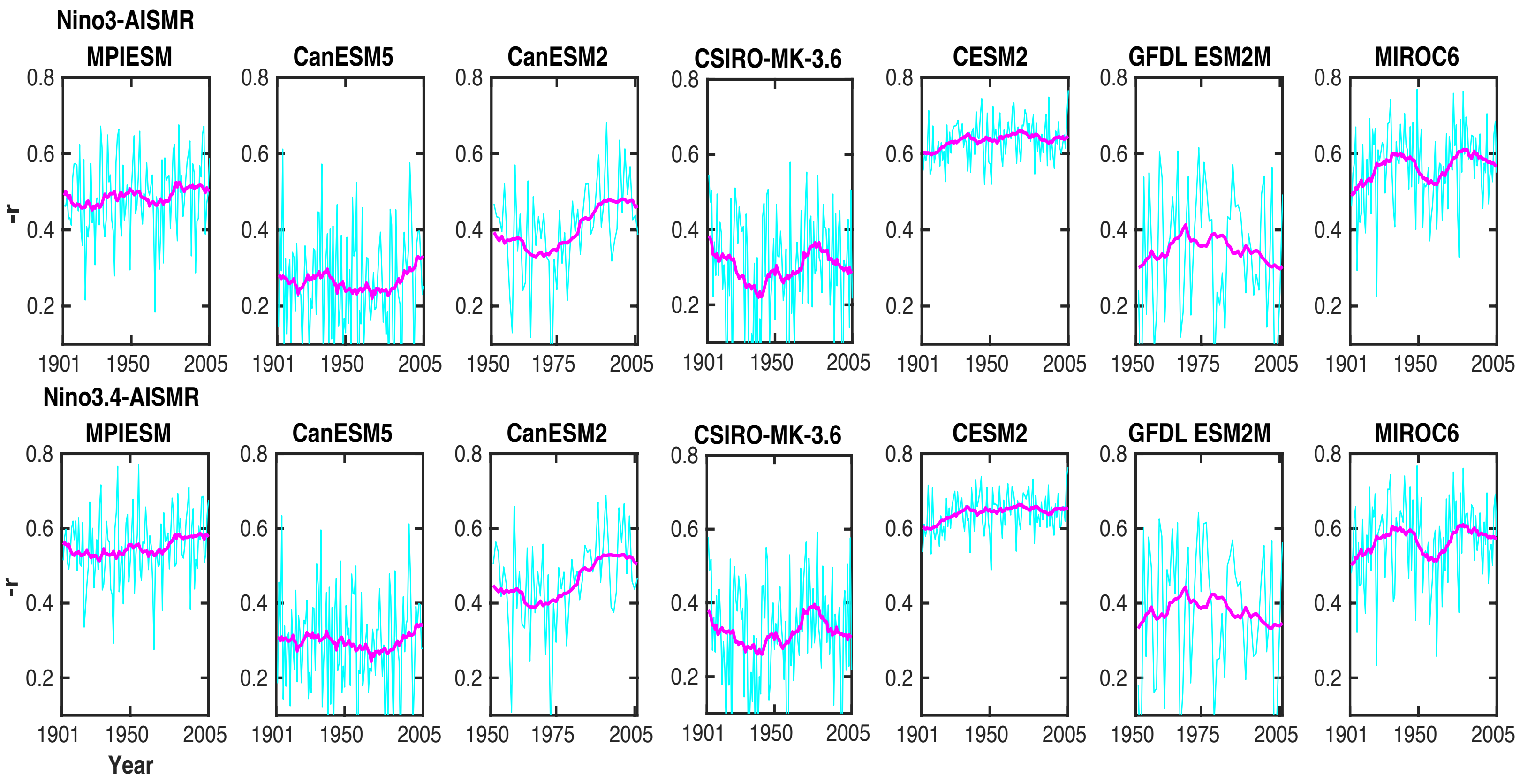

- None of the models shows a significant weakening of teleconnection at the end of 20th century.
- This shows that the role of external forcing is relatively weak in the observed weakening of ENSO-ISM teleconnection at the end of 20th century, and internal variability might have played a crucial role in it. This result is in agreement with Li and Ting 2015.

Fig: Top row displays the time-evolution of ensemble-wise correlation coefficients (r), between Nino3 SST and AISMR during 1901-2005 period. Magenta curve shows 21-year moving mean and cyan curve shows the yearly values. Bottom row is same as top, but for Nino 3.4 SST.

EOF Pattern and Variability of Pacific SST

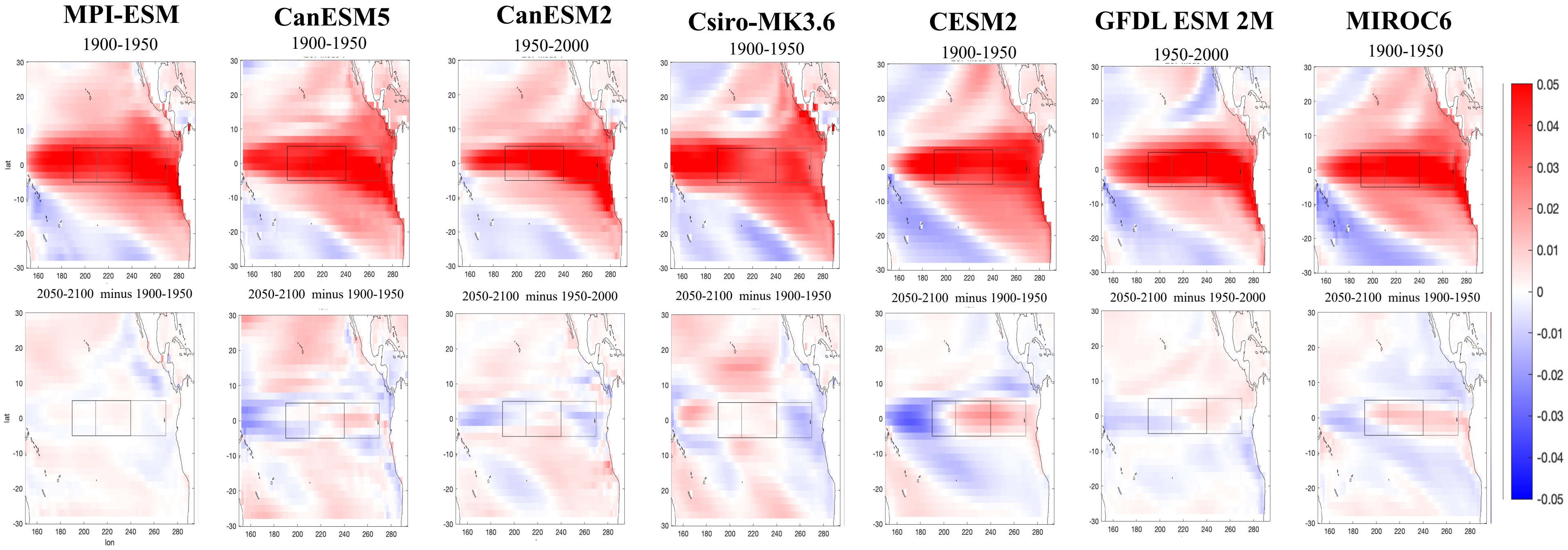

Fig1: Top row displays the EOF1 pattern (JJA) of SST over Pacific Ocean during 1900-1950/1950-2000. Bottom row shows the difference, 2050-2100 minus 1900-1950 or 1950-2000.

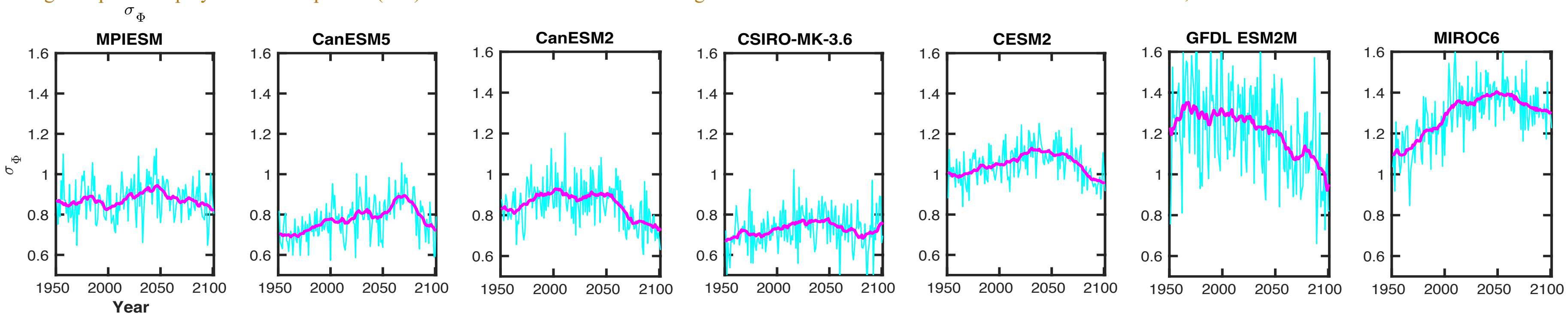

Fig2: Shows the ensemble-wise standard deviation of Nino3 SST during the JJA season. Magenta curve shows 21-year moving mean and cyan curve shows the yearly values.

- EOF1 pattern looks similar to the results in the literature. Furthermore, the forced change is very weak in model and other models shows significant variabilities.
- In the second half of 20th century and first half of 21st century ENSO variability increases in most of the models. While, under strong future forcing scenarios (late 21st century), typically ENSO variability starts to decline in a nonmonotonic, nonlinear fashion.

The Forced Evolution of Correlation Coefficients:

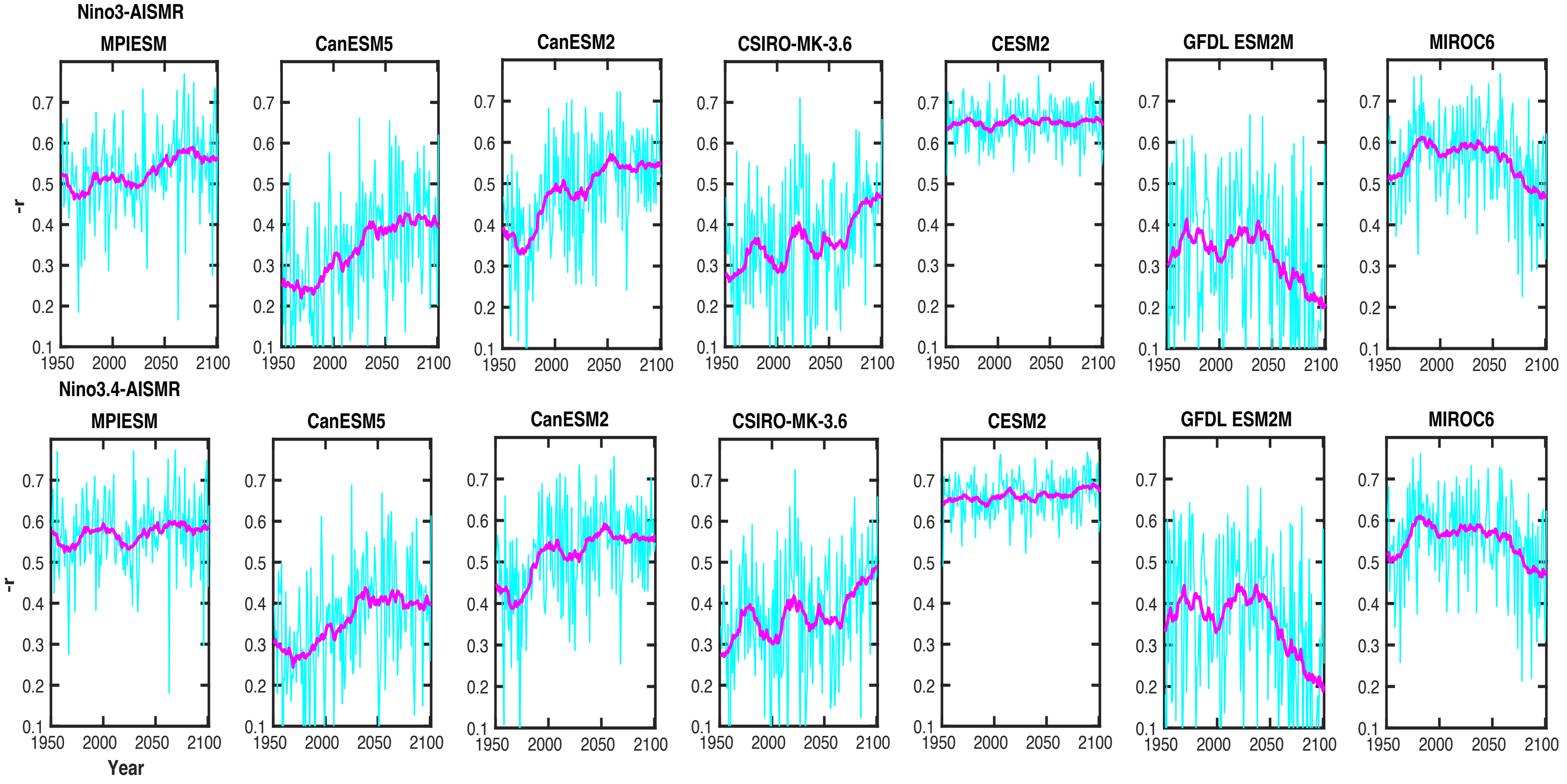

Fig: Top row displays the time-evolution of ensemble-wise correlation coefficients (r), between Nino3 SST and AISMR during 1950-2100 period. Magenta curve shows 21-year moving mean and cyan curve shows the yearly values. Bottom row is same as top, but for Nino 3.4 SST.

- Under moderate, historical and early 21st century, forced change of ENSO-ISM teleconnection is strengthening or nondecreasing in all the models.
- In the second half of 21st century, the teconnection strengthening or non-decreasing in 5 models and a weakening is observed in GFDL ESM 2M and MIROC6 models.

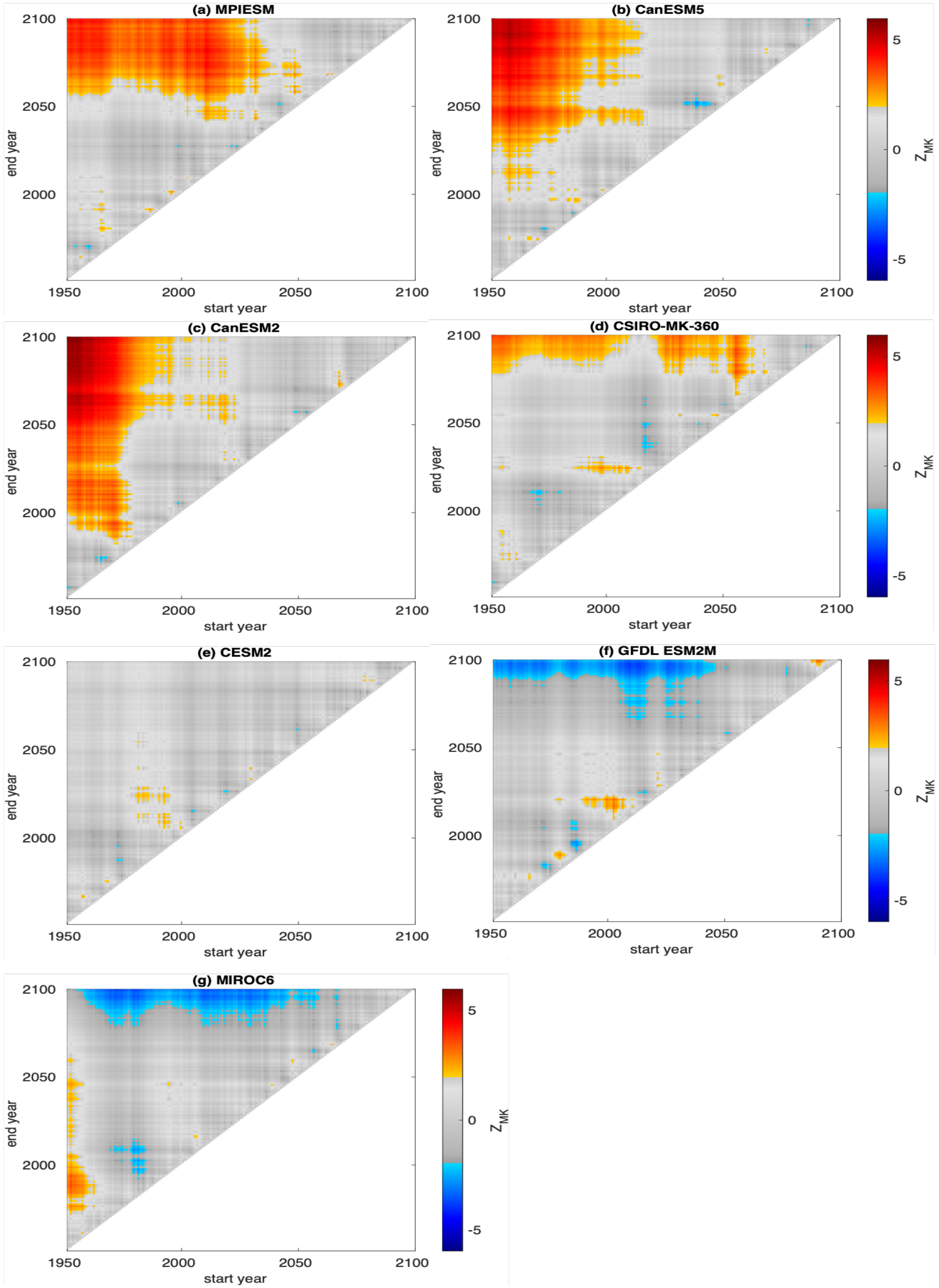

- The strengthening of ENSO-ISM teleconnection observed in MPIESM, CanESM5, CanESM2 CSIRO-MK-360, in the second half end of 21st century are statistically significant. While, CESM2 doesn't show any significant change.
- The late 21st century weakening of teleconnection observed in GFDL ESM 2M and MIROC6 models are significant.

FIG: Test statistics of the Mann-Kendall test for the stationarity of correlation coefficient. Red and blue shades correspond to $p < 0.05$, i.e., a detection of nonstationarity at that significance level.

Decomposition of the Forced Change of the Teleconnection Strength

In a regression analysis framework we identify three drivers of the teleconnection change:

(i) ENSO variability

(ii) ENSO-ISM coupling strength and

(iii) noise strength.

We attribute any strengthening of the teleconnection to (i)-(ii), namely, increasing ENSO variability and ENSO- ISM coupling strength

Regression Equation

$$\Psi = a\Phi + \xi,$$

$$r = \frac{a\sigma_\Phi}{\sigma_\Psi}$$

$$r = \frac{1}{\sqrt{1 + \left(\left(\sigma_\xi / \mathrm{a}\right)/\sigma_\Phi\right)^2}}$$

- The ENSO variability $\sigma_\Phi = \mathrm{std}[\Phi]$;
- The ENSO-IM coupling a, being the regression coefficient;
- The noise strength $\sigma_\xi = \mathrm{std}[\xi]$.

Bodai et al., 2021

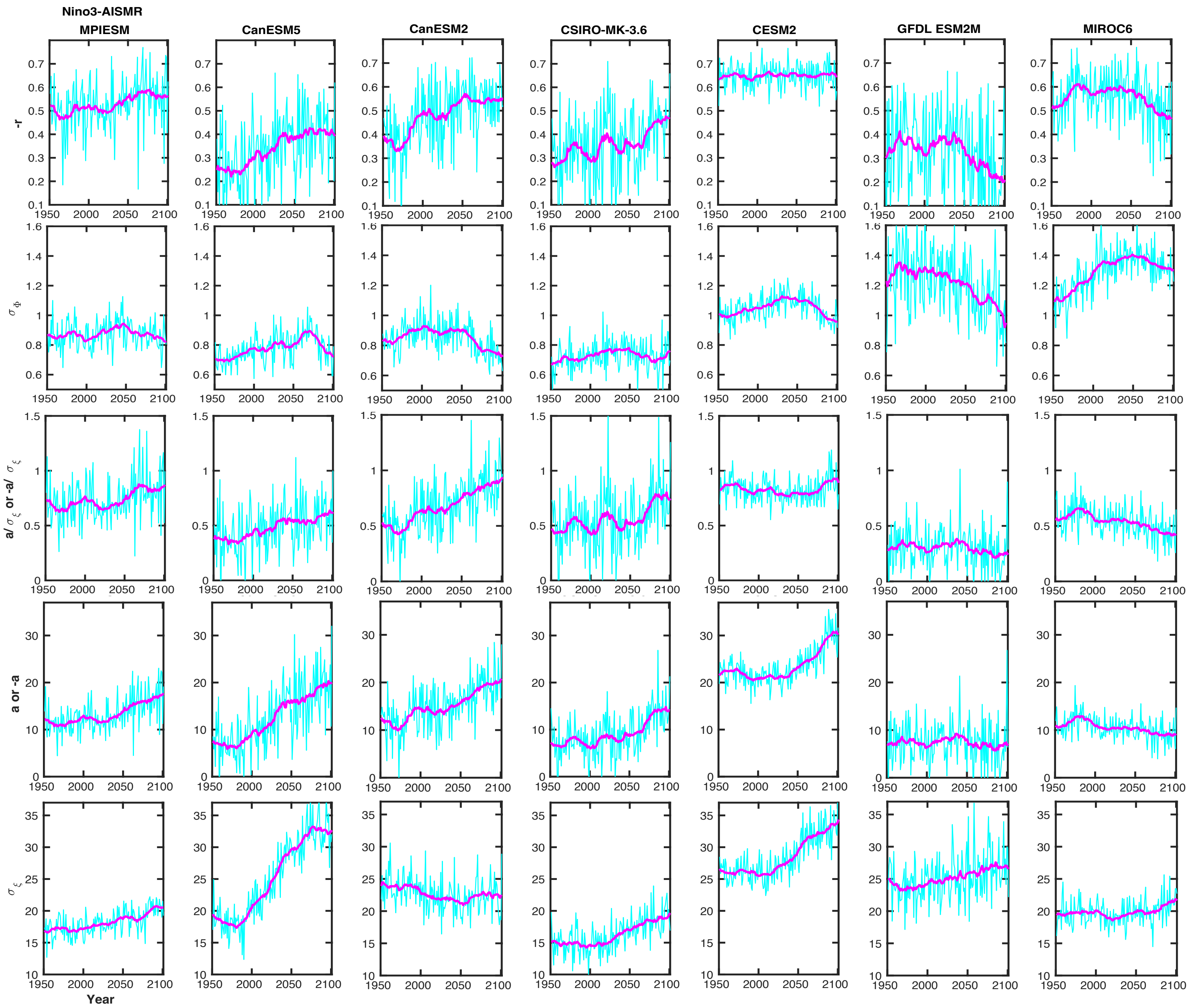

- The non-decreasing teleconnection strength in the early and middle part of 21st century is due to an increasing ENSO variability as well as coupling strength.
- This non-increasing nature of coupling strength and decreasing ENSO variability, played a dominant role in the weakening of the ENSO-ISM teleconnection in GFDL ESM 2M and MIROC6 models under strong late 21st century forcing.

Spatial Pattern of Correlation Coefficient and its Forced Change

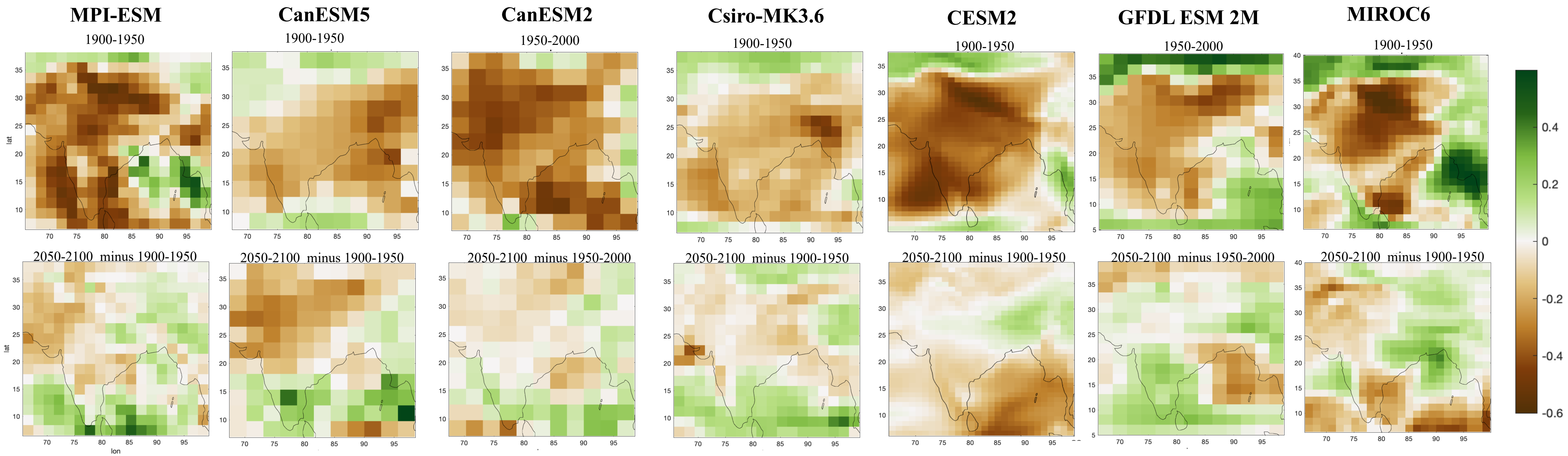

- The spatial pattern of the forced response of ENSO-ISM teleconnection shows an east-west dipole pattern over north-India, in most of the models. However, there is no inter-model robustness in the south India.

Summary

- The forced response of the teleconnection between the ENSO and the Indian summer monsoon (ISM) evaluated using a multi-model ensemble of initial conditional ensembles under historical forcing and future (RCP8.5/SSP5-8.5/SSP3-7.0) forcing scenarios.
- The role of external forcing is relatively weak in the observed weakening of ENSO-ISM teleconnection at the end of 20th century, internal variability might have played a crucial role in it.
- In the early and middle part of the 21st century that the teleconnection is strengthening or nondecreasing. This considerable robustness is owing to an increasing ENSO variability as well as coupling strength.
- In the end of the 21st century, there is no inter-model robustness in the projected teleconnection. This is mainly due to the ENSO variability change is not projected robustly across models: either the start of the ENSO variance decline is not captured robustly, or the rates of the decline of ENSO variance competing this time with an increase of the coupling strength.


thank you

EOF Pattern and Variability of ISM Rainfall

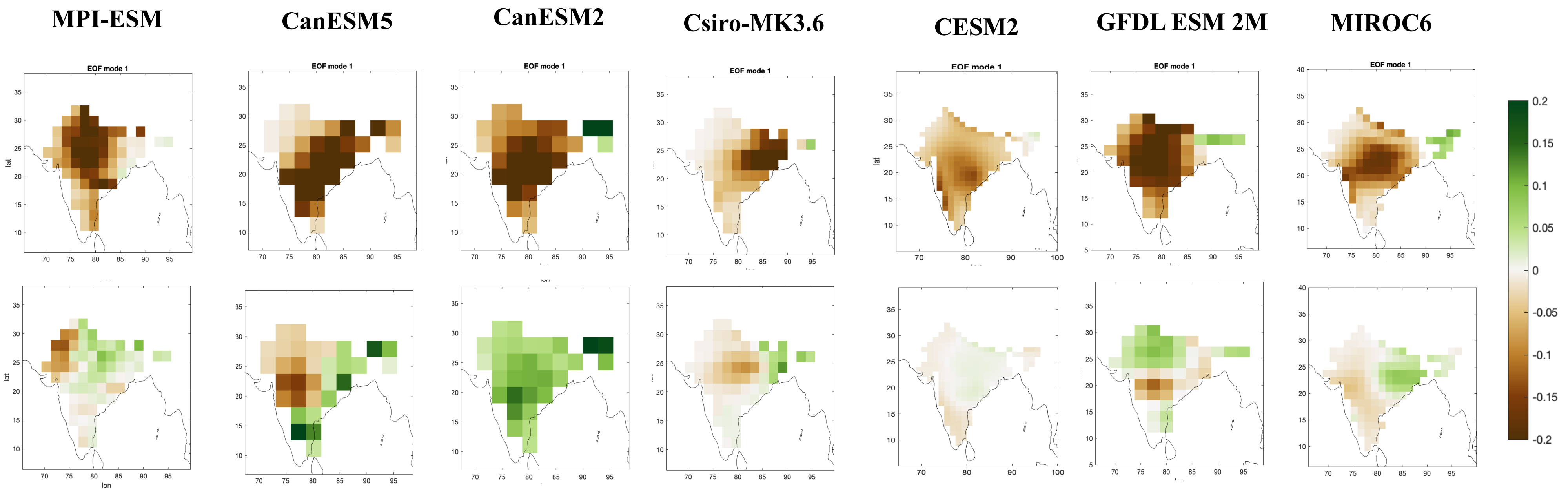

Fig1: Top row displays the EOF1 pattern (JJAS) of ISM rainfall during 1900-1950 or1950-2000. Bottom row shows the EOF1 pattern difference, 2050-2100 minus 1900-1950 or 1950-2000.

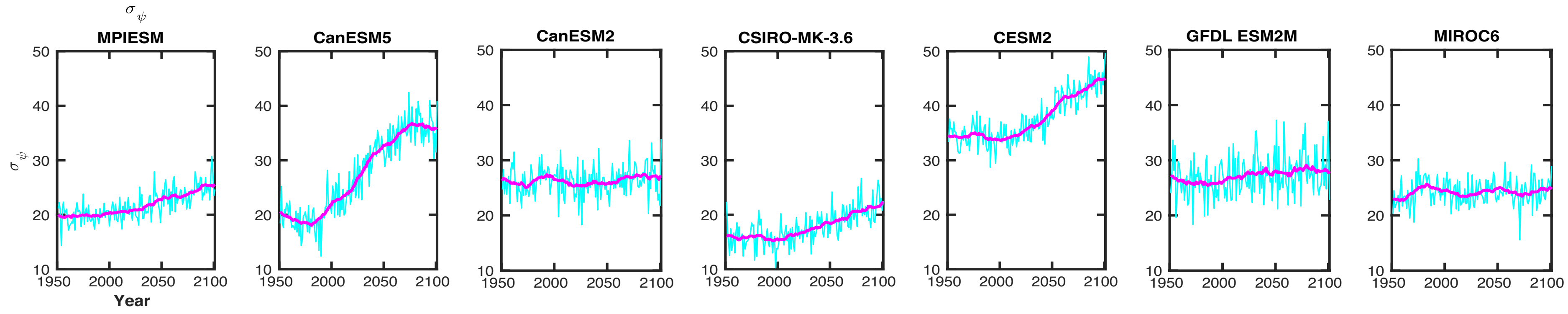

Fig2: Shows the ensemble-wise standard deviation of ISM rainfall during the JJAS season. Magenta curve shows 21-year moving mean and cyan curve shows the yearly values.

- The spatial pattern of the forced response of ISM rainfall shows an east-west dipole pattern over north-India, in most of the models (except CanESM2 and GFDL ESM 2M).
- Under future forcing scenarios, the ensemble-wise variance of ISM rainfall increases in MPIESM, CanESM5, Csiro MK 3.6 and CESM2 models. Hardly any forced change is observed in the other three models.